Contents lists available at ScienceDirect

Cancer Letters

Original Articles

Novel flexible heteroarotinoid, SL-1-39, inhibits HER2-positive breast cancer cell proliferation by promoting lysosomal degradation of HER2

Hongye Zou[a], Mary B. Sevigny[a], Shengquan Liu[b], David T. Madden[b,c], Maggie C. Louie[a,b,*]

[a] Department of Natural Sciences and Mathematics, Dominican University of California, 50 Acacia Avenue, San Rafael, CA, 94901, USA
[b] College of Pharmacy, Touro University California, 1310 Club Drive, Vallejo, CA, 94594, USA
[c] Buck Institute for Research on Aging, 8001 Redwood Boulevard, Novato, CA, 94945, USA

ABSTRACT

SL-1-39 [1-(4-chloro-3-methylphenyl)-3-(4-nitrophenyl)thiourea] is a new flexible heteroarotinoid (Flex-Het) analog derived from the parental compound, SHetA2, previously shown to inhibit cell growth across multiple cancer types. The current study aims to determine growth inhibitory effects of SL-1-39 across the different subtypes of breast cancer cells and delineate its molecular mechanism. Our results demonstrate that while SL-1-39 blocks cell proliferation of all breast cancer subtypes tested, it has the highest efficacy against HER2 + breast cancer cells. Molecular analyses suggest that SL-1-39 prevents S phase progression of HER2 + breast cancer cells (SKBR3 and MDA-MB-453), which is consistent with reduced expression of key cell-cycle regulators at both the protein and transcriptional levels. SL-1-39 treatment also decreases the protein levels of HER2 and pHER2 as well as its downstream effectors, pMAPK and pAKT. Reduction of HER2 and pHER2 at the protein level is attributed to increased lysosomal degradation of total HER2 levels. This is the first study to show that a flexible heteroarotinoid analog modulates the HER2 signaling pathway through lysosomal degradation, and thus further warrants the development of SL-1-39 as a therapeutic option for HER2 + breast cancer.

1. Introduction

The human epithelial receptor 2 (HER2 or erbb2) is a member of the epidermal growth factor receptor (EGFR) family of receptor tyrosine kinases that act through the EGF signaling cascade [1,2]. Approximately 20% of breast cancers overexpress HER2 and consequently, are referred to as HER2-positive (HER2 +) breast cancer [3–6]. The dysregulation of the HER2/EGFR pathway has been shown to result in uncontrolled growth that can contribute to cancer progression [7,8]. The phosphorylation of the HER2 receptor dimers subsequently activates several downstream pathways, including the PI3K (phosphatidylinositol-3-kinase)/Akt (protein kinase B) pathway and the Ras-Raf (rapidly accelerated fibrosarcoma)-MAPK (mitogen-activated protein kinases) pathway [2,9]. These two pathways further modulate cell proliferation, migration, angiogenesis, invasion, apoptosis and other cellular processes [10,11]. Interestingly, unlike other EGFR members, HER2 does not have a specific ligand binding domain and therefore is constitutively active [12]. As a result, HER2 easily interacts with other activated EGFR receptors, making HER2 the preferred dimerization partner for these receptors and consequently an ideal target for breast cancer therapies [13–15].

Amongst the newest cancer therapies being developed are flexible heteroarotinoids (Flex-Hets), which are derived from retinoids and possess promising anti-cancer activity [16–19]. Studies have shown that one of the first Flex-Hets developed, SHetA2, inhibits growth of the National Cancer Institute's panel of 60 human tumor cell lines by regulating apoptosis, cell growth, differentiation and angiogenesis [17,19–21]. However, compared to most drugs, SHetA2 has higher lipophilicity (logP = 7.09) [22] which may limit its bioavailability [23]. Therefore, a 2nd generation of Flex-Hets was designed and synthesized to retain the anti-cancer activity of SHetA2 but with lower lipophilicity [22].

The current study aims to investigate the effects of SL-1-39— a promising 2nd generation analog of SHetA2— on breast cancer cell growth. This is the first study to show that a flexible heteroarotinoid blocks HER2 + breast cancer cell growth by disrupting the EGFR/HER2 pathway. In particular, we demonstrate that SL-1-39 treatment in HER2 + breast cancer cells leads to lysosomal degradation of HER2. Our results strongly support further development of SL-1-39 as a therapeutic option for HER2 + breast cancer and underscore the importance

---

* Corresponding author. Department of Natural Sciences and Mathematics, Dominican University of California, 50 Acacia Avenue, San Rafael, CA, 94901, USA.
E-mail addresses: zou3178635@gmail.com (H. Zou), mary.sevigny@dominican.edu (M.B. Sevigny), shengquan.liu@tu.edu (S. Liu),
david.madden.tu@gmail.com (D.T. Madden), maggie.louie@dominican.edu (M.C. Louie).

of studying the effects of flexible heteroarotinoids, like SL-1-39, on other cancer types that overexpress HER2 and/or members of the EGFR family.

2. Materials and methods

2.1. Cell culture

Breast cancer cell lines MCF-7, T47D, SKBR3, MDA-MB-453, BT474, MDA-MB-468, MDA-MB-231, HCC1806 and BT20 and the normal breast cell line MCF-10A were obtained from the American Type Culture Collection (ATCC; Manassas, VA). Details of cell maintenance are found in the supplemental methods.

2.2. Growth assay

Approximately 2×10^3 cells per well were plated in a 96-well plate and cells were either treated with the drug at different concentrations (0.5, 1.0, 5.0, 10.0, and 20.0 μM) or mock treated with the vehicle (DMSO; Sigma-Aldrich, St. Louis, MO) for 48 h. For long term growth assay, cells were treated with 2.5 and 5 μM of SL-1-39 or mock-treated with DMSO for two, three and four days. Cell proliferation was monitored with MTT (Life Technologies, Carlsbad, CA) per manufacturer's protocol.

2.3. Cell viability and apoptosis assay

The Apolive-Glo™ Multiple Assay (Promega, Sunnyvale, CA) was used to evaluate cell viability and apoptosis. Cells were plated at 1000 cells per well in a 96-well plate (Corning, Corning, NY) and treated with one of the following: 5 μM SHetA2, SL-1-39, 10 μM digoxin, 100 nM cabazitaxel or mock treated with DMSO. Forty-eight hours after treatment, analysis was performed per manufacturer's protocols using a FLUOstar® Omega microplate reader (BMG Lab Tech lnc., Cary, NC).

2.4. Bromodeoxyuridine (BrdU) incorporation assay

Approximately 2×10^5 cells were plated in 6-well plates containing glass coverslips. Cells were treated with 2.5 or 5 μM SL-1-39 or mock-treated 24 h later. One hour prior to harvesting the cells (12, 24 and 48 h post-treatment), cells were pulse-labeled with 10 μM BrdU for 1 h. Cells were fixed with 10% formalin in phosphate buffer saline (PBS), and BrdU-positive cells were analyzed as previously published [24] and briefly described in the supplemental methods.

2.5. Protein and gene expression analysis

For protein expression, cells were lysed in buffer containing 0.05M HEPES, 1% Triton, 0.1% SDS, 0.002M EDTA, 1% deoxycholate, 0.002M EGTA, 0.15M NaCl, 0.01M NaF, and 1% Halt™ protease inhibitor cocktail (Thermo-Fisher Scientific, Waltham, MA) and protein expression was analyzed using western blot analysis. Details of protocol and list of antibodies are found in the supplemental methods. For gene expression, total RNA was isolated via Direct-zol RNA kit according to the manufacturer's protocol (Zymo Research Corporation, Irvine, CA). RNA was converted to cDNA using oligo-dT$_{18}$ primers and Moloney Murine Leukemia Reverse Transcriptase (MMLV-RT; Promega). Gene expression was monitored via semi-quantitative or quantitative RT-PCR (qRT-PCR) using Go-Taq Green Master Mix (Promega) or Fast SYBR™ Green Master Mix, respectively (Life Technologies, Carlsbad, CA). Relative mRNA expression was normalized to GAPDH. All primers were synthesized by Integrated DNA Technologies, Inc. (San Diego, CA) and sequences are found in the supplemental methods.

2.6. Immunofluorescence

Approximately 2×10^5 SKBR3 cells were plated in 6-well plates containing glass coverslips. The cells were treated with 5 μM SL-1-39 or mock-treated 24 h later. After 22 h of treatment, cells were exposed to 20 or 50nM of Bafilomycin for 2 h. Cells were fixed with 10% formalin in PBS and permeabilized with 1X PBS + 0.5% Triton for 30 min at room temperature. Slides were blocked with PBS + 10% FBS and incubated with anti-Lamp1 (D2D11, Cell Signaling, Danvers, MA) and anti-HER2 (3B5, Santa Cruz Biotechnology) in PBS for 2 h at 37 °C. Slides were washed twice with PBS, incubated with Alexa Fluor-conjugated secondary antibodies (Life Technologies) for 2 h at room temperature, washed twice with PBS, and mounted with Prolong Gold with DAPI (Life Technologies). Images were captured at 2048 × 2048 resolution on a Zeiss LSM-700 confocal microscope using a 40X oil objective. For each region of interest, five z-stacks were captured and subsequently processed with ImageJ (https://imagej.nih.gov/ij/) to produce z-projections and to adjust brightness and contrast.

2.7. Statistical analysis

All statistical analyses were conducted using GraphPad Prism 6 (Graphpad Software Inc., La Jolla, California). The best-fit IC$_{50}$ curves were fitted to one-phase decay or sigmoidal dose-response algorithms. All results are presented as mean ± SD.

3. Results

3.1. SL-1-39 reduces breast cancer cell proliferation by preventing S-phase progression

To understand the effects of SL-1-39 on breast cancer, we evaluated the growth inhibitory activity of SL-1-39 on a panel of breast cancer cells including MCF7, T47D, MDA-MB-231, MDA-MB-453, MDA-MB-468, SKBR3, HCC1806 and BT20 (Table 1). Results in Table 1 establish that SL-1-39 effectively decreased the growth of most breast cancer cells with an IC$_{50}$ ranging from 2.20 to 5.53 μM. Amongst the cell lines tested, the ER-/HER2+ MDA-MB-453 and SKBR3 cells showed the greatest sensitivities to SL-1-39, with IC$_{50}$ values of 2.20 ± 1.13 μM and 2.91 ± 0.91 μM, respectively.

To determine whether the growth inhibitory effects of SL-1-39 were sustained beyond two days, SKBR3 and MDA-MB-453 were treated with either 2.5 or 5 μM of SL-1-39 (or mock-treated), and cell growth was evaluated two, three, and four days after treatment (Fig. 1A–B). Consistent with the data in Table 1, both concentrations of SL-1-39 inhibited SKBR3 and MDA-MB-453 cells two days post-treatment, and this inhibitory effect was sustained for four days without further addition of the drug. To elucidate how SL-1-39 blocks cell growth, a BrdU incorporation assay was used to evaluate SL-1-39's effect on S-phase progression. Breast cancer cells were treated with 2.5 or 5 μM of SL-1-39 or mock-treated, pulse-labeled with BrdU for 1 h, and then collected

Table 1
Potency of SL-1-39 in different breast cancer cell lines.
Potency (IC$_{50}$ values) in μM (mean ± SD).

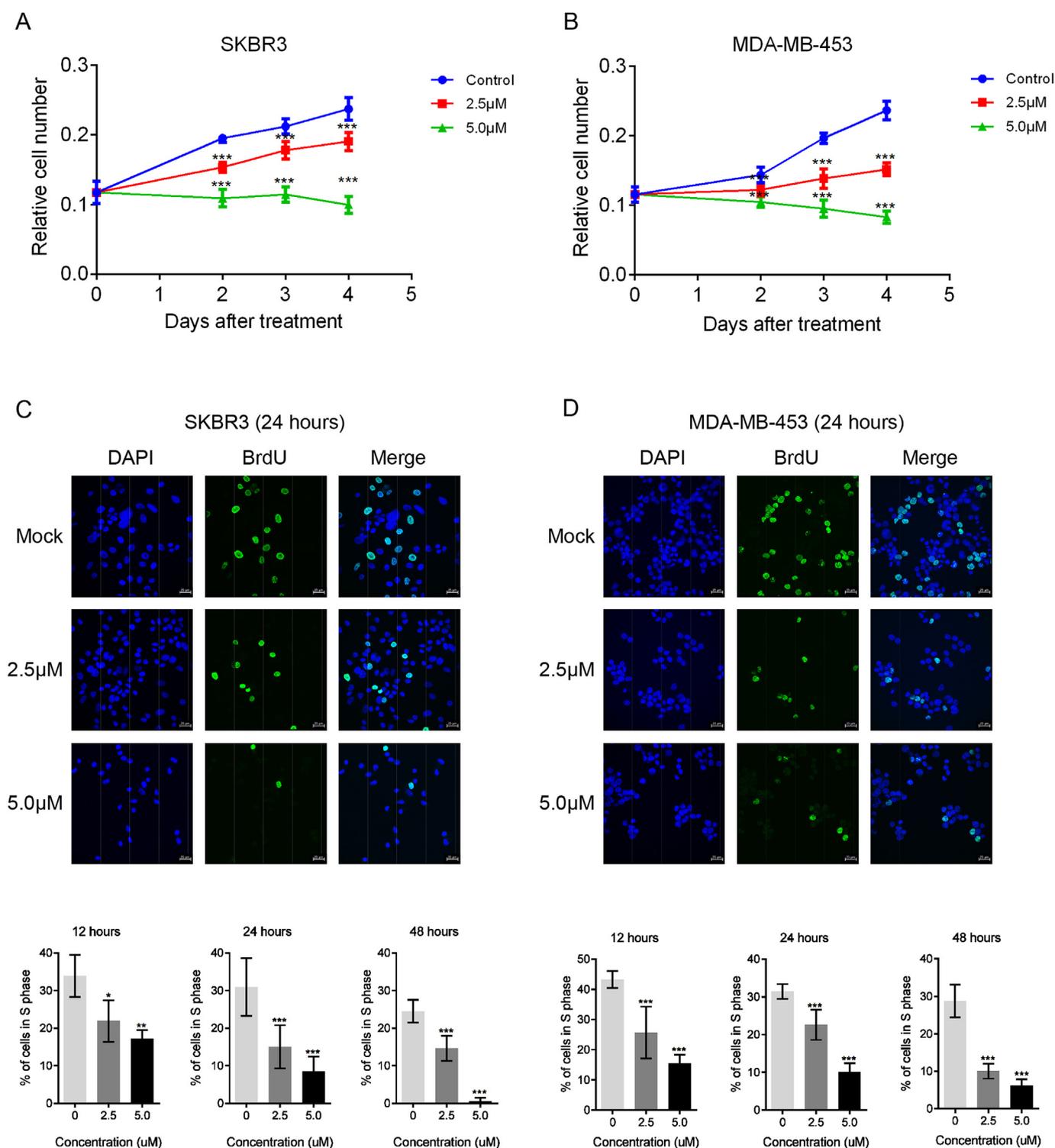| Breast cancer cell lines	Cell type	SL-1-39 IC50 values in μM (mean ± SD)
MCF7	Luminal-type	5.53 ± 1.11
T47D	Luminal-type	3.06 ± 1.40
SKBR3	Luminal-type	2.91 ± 0.91
MDA-MB-453	Luminal-type	2.20 ± 1.13
MDA-MB-468	Basal-type	3.47 ± 0.33
MDA-MB-231	Basal-type	5.47 ± 1.15
HCC1806	Basal-type	5.37 ± 0.30
BT20	Basal-type	3.41 ± 1.22

Fig. 1. **SL-1-39 reduced ER-negative breast cancer cell proliferation up to 4 days by preventing cells into S phase.** SKBR3 (A) and MDA-MB-453 (B) cells were plated in 96-well plates and treated with 2.5 μM, 5 μM SL-1-39 or mock treated. Relative cell numbers were determined using MTT 2, 3, 4 days after treatment (***, P < 0.001). SKBR3(C) and MDA-MB-453(D) cells were seeded on coverslips in 6-well plates and treated with 2.5 μM, 5 μM SL-1-39 or mock treated. After 12, 24 and 48 h, cells were stained with BrdU, fixed and then analyzed on a fluorescent microscope. Nuclei were visualized by DAPI staining (in blue). Cells undergoing DNA synthesis appeared in green (BrdU). Columns represent the percentage of cells in S phase with SD (*, P < 0.05; **, P < 0.01; ***, P < 0.001). Experiments were repeated at least three times.

12, 24, and 48 h after treatment. Cells treated with 2.5 μM and 5 μM of the analog for 24 h showed not only a decrease in total cell number but also a decrease in the percentage of cells in S-phase, as noted by the reduction in BrdU-positive cells (Fig. 1C and D). Quantitative analysis confirmed that even as early as 12 h the number of SKBR3 cells in S-

phase decreased from 33.8% in mock-treated cells to 21.9% and 17.1% in cells treated with 2.5 μM (P < 0.05) and 5 μM (P < 0.01) of SL-1-39, respectively (Fig. 1C). Forty-eight hours after 5 μM SL-1-39 treatment, less than 2% of the SKBR3 cells were in S-phase (P < 0.001). Similar results were observed in MDA-MB-453 cells, with the
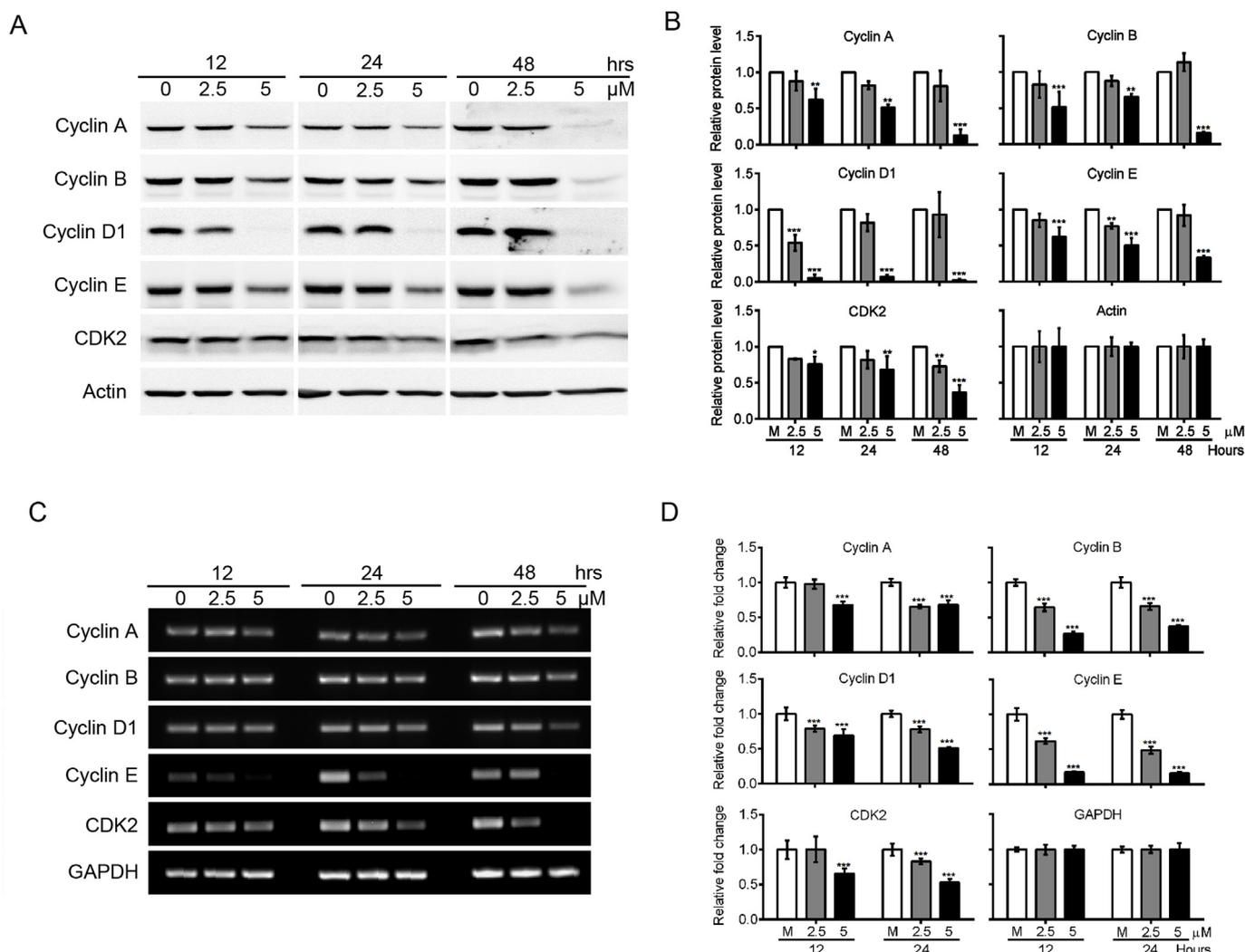
A

B

C

D

Fig. 2. SL-1-39 reduced the expression of cell cycle regulators. MDA-MB-453 cells were plated in 6-well plates and treated with 2.5 μM, 5 μM SL-1-39 or mock treated for 12, 24 or 48 h. (A) cyclin A, cyclin B, cyclin D1, cyclin E and CDK2 protein expressions in cell lysates were analyzed with western blot. Actin served as control. (B) Quantification of western blot, columns represent average protein expression level (with SD) of at least three independent experiments (*, P < 0.05; **, P < 0.01; ***, P < 0.001). (C) RT-PCR analysis of cyclin A, cyclin B, cyclin D1, cyclin E and CDK2 in total RNA extracted from cell lysates. GAPDH served as control. (D) Real-time PCR analysis of cyclin A, cyclin B, cyclin D1, cyclin E and CDK2 in total RNA extracted from cell lysates. GAPDH served as control. (***, P < 0.001).

percentage of cells in S-phase decreasing from 43.2% in mock-treated cells to 25.7% and 15.4% in cells treated for 12 h with 2.5 μM and 5 μM of SL-1-39, respectively (P < 0.001) (Fig. 1D). After 48 h of 5 μM SL-1-39 treatment, only 6.2% of the cells were in S-phase (P < 0.001).

MDA-MB-453 and SKBR3 cells were also treated with either SL-1-39 or SHetA2 to evaluate the induction of apoptosis (Fig.S1). A subset of cells was treated with either digoxin, a Na+/K+ ATPase inhibitor, or cabazitaxel, a chemotherapeutic drug that targets microtubule poly-merization, to serve as positive controls for apoptosis. As expected, SL-1-39, SHetA2, digoxin and cabazitaxel reduced MDA-MB-453 and SKBR3 cell growth by at least 2.5-fold (Fig.S1A and C). However, while digoxin and cabazitaxel significantly increased activities of caspase 3 and 7, important markers of apoptosis [25,26], SL-1-39 and ShetA2 did not (Fig. S1B and D). The data suggest that the decrease in growth of ER-breast cancer cells is associated with an inhibition of cell pro-liferation, not an increase in apoptosis. We also tested SL-1-39 and SHetA2 on human mammary epithelial cells (HMECs). Results show that while these heteroarotinoids do dcrease the growth of HMECs, the compounds do not induce apoptosis (Fig.S1E and F).

3.2. SL-1-39 decreases the expression of cell cycle regulators

Since SL-1-39 appears to block S-phase progression, the expression levels of key cell cycle regulators were analyzed in MDA-MB-453 and SKBR3 cells using western blot analysis (Fig. 2 and Fig.S2). Results show that in MDA-MB-453 cells, 5 μM of SL-1-39 was sufficient to re-duce the expression of cyclin A (P < 0.01), cyclin B, cyclin D1, and cyclin E (P < 0.001) within 12 h of treatment and cdk2 (P < 0.01) by 24 h (Fig. 2-B). These decreases were still observed 48 h after treatment. Amongst all the cell cycle proteins analyzed, cyclin D1 was the most impacted, with protein levels dropping by 95% in cells treated with 5 μM of SL-1-39 for 48 h (Fig. 2B).

To determine if a similar decrease is also observed at the mRNA level, semi-quantitative and quantitative RT-PCR (qRT-PCR) were used to analyze the transcript levels of cell cycle genes in MDA-MB-453 cells treated as previously described. Cells treated with SL-1-39 expressed lower levels of several cell cycle genes at the mRNA level (Fig. 2C–D). Quantitative RT-PCR data indicate that MDA-MB-453 cells treated with 5 μM of SL-1-39 expressed significantly less cyclin A, B, D1, E, and cdk2 12 h after treatment (32%, 73%, 31%, 83% and 35%, respectively; P < 0.001; Fig. 2D). Furthermore, the mRNA levels of cyclin B, cyclin

A

B
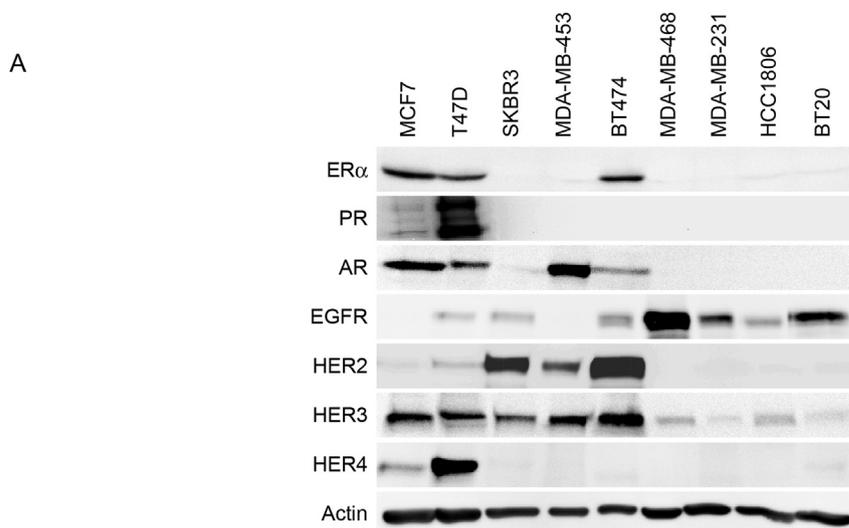
breast cancer cell lines	Cell type	Characteristic	IC50	ERα	PR	AR	EGFR	HER2	HER3	HER4
MCF7	Luminal-type	ER+/PR+	5.53±1.11	++	+	+++	-	-	++	+
T47D	Luminal-type	ER+/PR+/HER2+	3.06±1.40	++	++++	++	+	+	++	++++
SKBR3	Luminal-type	HER2+	2.91±0.91	-	-	-	+	++++	++	-
MDA-MB-453	Luminal-type	HER2+	2.20±1.13	-	-	+++	-	++	++	-
BT474	Luminal-type	ER+/HER2+	2.39±0.28	++	-	+	+	++++	+++	-
MDA-MB-468	Basal-type	TNBC	3.47±0.33	-	-	-	++++	-	+	-
MDA-MB-231	Basal-type	TNBC	5.47±1.15	-	-	-	++	-	-	-
HCC1806	Basal-type	TNBC	5.37±0.30	-	-	-	+	-	+	-
BT20	Basal-type	TNBC	3.16±1.22	-	-	-	+++	-	-	-

Fig. 3. SL-1-39 response is associated with HER2 expression. (A) Receptor expression (ERα, PR, AR, EGFR, HER2, HER3, HER4) in total cell lysates (MCF7, T47D, SKBR3, MDA-MB-453, BT474, MDA-MB-468, MDA-MB-231, HCC1806 and BT20) were analyzed with western blot. Actin served as control. (B) Breast cancer cell lines with their SL-1-39 response and expression status of biomarkers.

D1 and cyclin E were decreased with only 2.5 μM of SL-1-39 12 h after SL-1-39 treatment (P < 0.001). The inhibitory effects of SL-1-39 on the cell cycle regulators were also confirmed in SKBR3 cells (Fig.S2A-B), albeit a more modest effect was observed. Coupled with the growth data, the results clearly suggest that SL-1-39 inhibits breast cancer cell growth by decreasing the expression of key cell cycle regulators at both protein and mRNA levels.

3.3. SL-1-39 reduces HER2 expression and inhibits the EGFR/HER2 signaling pathways

To further investigate the mechanism of action of SL-1-39, western blot analysis was used to determine the expression of important breast cancer biomarkers— ERα, PR, AR, EGFR (HER1), HER2, HER3 and HER4— in all the breast cancer cell lines previously found to respond to

SL-1-39 treatment (Fig. 3A). This analysis confirmed the following: MCF7, T47D and BT474 are ERα+; T47D, SKBR3, MDA-MB-453 and BT474 are HER2+; and MDA-MB-468, MDA-MB-231, HCC1806 and BT20 are ERα-, PR-, and HER2- (triple negative breast cancer cell lines). For each cell line, the expression status of each biomarker was compared to its SL-1-39 response using IC_{50} values (Fig. 3B). Interestingly, cells expressing HER2 collectively exhibited a greater sensitivity towards SL-1-39. T-47D, SKBR3, MDA-MB-453 and BT474 all express HER2, and the IC_{50} values are 3.06 ± 1.40 μM, 2.91 ± 0.91 μM, 2.20 ± 1.13 μM and 2.39 ± 0.28 μM, respectively. The correlation of HER2 expression to IC_{50} suggests that SL-1-39-mediated growth inhibition may involve modulating the HER2/EGFR signaling pathway.

To determine whether the HER2/EGFR pathway plays a role in mediating the effects of SL-1-39, we analyzed the protein expression status of HER2 and its downstream effectors, MAPK and Akt in MDA-
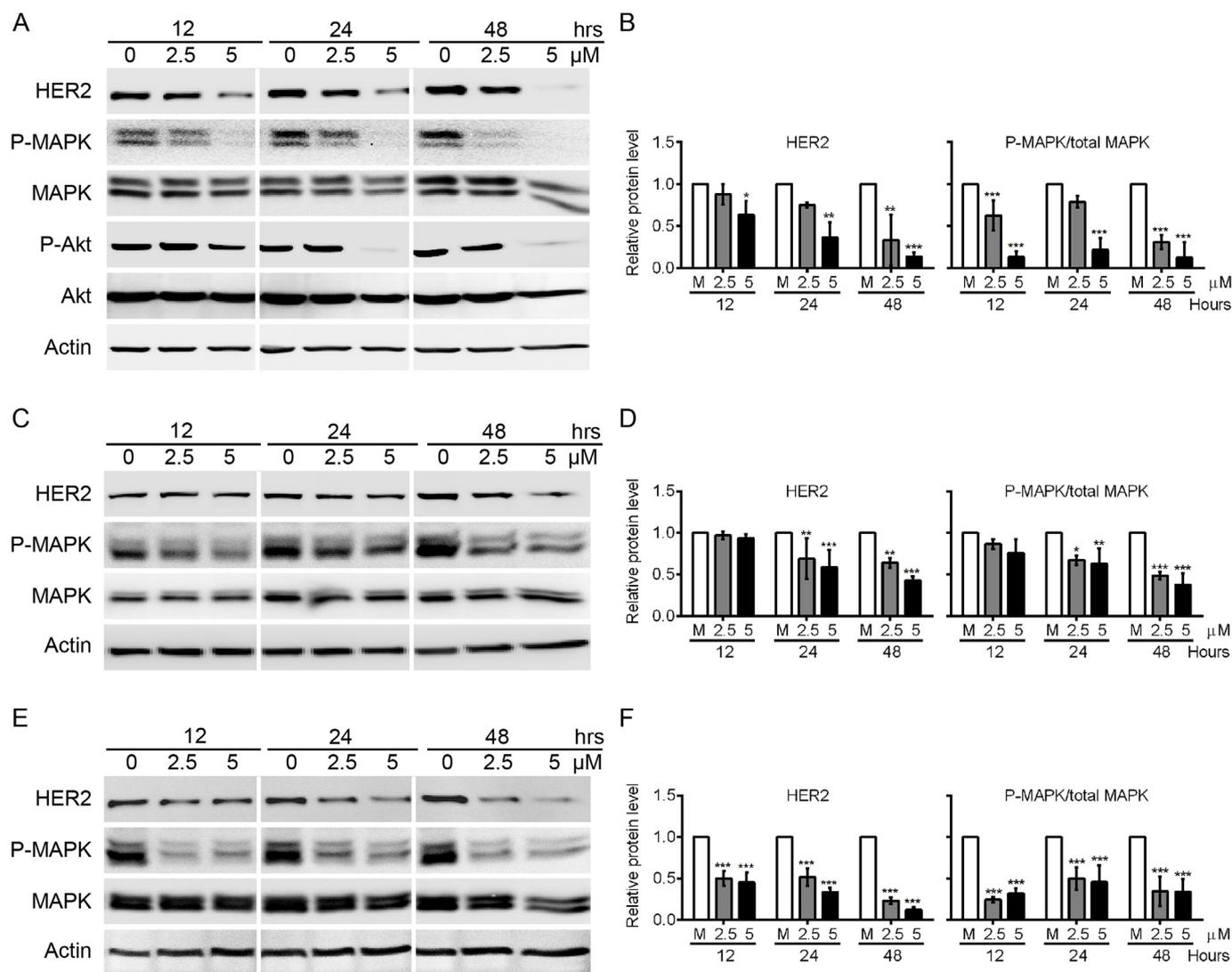
Fig. 4. SL-1-39 decreased HER2 expression and phosphorylation of HER2 downstream effectors. Cells were plated in 6-well plates and treated with 2.5 μM, 5 μM SL-1-39 or mock treated for 12, 24 or 48 h. HER2, P-MAPK, MAPK, P-Akt, Akt protein expressions in MDA-MB-453 (A), SKBR3 (C), T47D (E) cells were analyzed with western blots. Actin served as control. Quantification of HER2 expression and average ratio of P-MAPK/total MAPK were analyzed in MDA-MB-453 (B), SKBR3 (D), T47D (F) cells, data represent at least three independent experiments (*, $P < 0.05$; **, $P < 0.01$; ***, $P < 0.001$).

MB-453 cells treated with SL-1-39. Western blot data in Fig. 4A and B shows that in MDA-MB-453 cells a 36.7% decrease in HER2 protein expression occurred within 12 h of 5 μM SL-1-39 treatment; and after 48 h of treatment, the expression dropped 86.4% compared to control. Consistent with this observation, the level of phosphorylated MAPK, an important downstream effector of the HER2/EGFR signaling pathway, also showed significant reduction at 12 h, while the total MAPK level did not significantly decrease until 48 h.

After confirming that SL-1-39 reduces HER2 expression and MAPK phosphorylation in MDA-MD-453 cells, we questioned whether other HER2 positive breast cancer cells (SKBR3, T-47D and BT-474) have a similar response to SL-1-39. Consistent with the results seen in MDA-MB-453 cells, SKBR3, T-47D and BT-474 also exhibited lower expression of HER2 and pMAPK, particularly after 24 and 48 h of SL-1-39 treatment, while the total MAPK did not show any significant change (Fig. 4C and E, and Fig. S3). Quantification of western blots confirmed that after 24 h of 5 μM treatment of SKBR3 and T47D cells, HER2 protein levels dropped to 33.7% and 58.4% respectively, while the relative ratio of pMAPK to total MAPK was reduced by 36.9% and 54.3%, respectively ($P < 0.01$, Fig. 4D and F). Interestingly, SKBR3 exhibited only moderate levels of HER2 down-regulation though it has the

highest HER2 expression, while T47D, with its lower level of HER2 expression, showed a more significant reduction.

To evaluate whether the decrease in HER2 and P-MAPK expression occurred earlier than 12 h, MDA-MB-453 cells were treated with 5 μM SL-1-39 and collected at 2, 4, 8, 12 and 24 h after treatment (Fig. 5A). Similar experiments were carried out on SKBR3, which is amplified in HER2 (data not shown). Results in Fig. 5A show a reduction in both HER2 and the active phosphorylated form, P-HER2, as early as 2 h after treatment. Again, while the total expression of MAPK did not significantly change, levels of P-MAPK were dramatically reduced by 70.1% just 2 h after treatment ($P < 0.001$). We also analyzed Akt, another downstream kinase of the HER2 pathway; and results indicate that although total Akt levels did not show a significant decrease (except for a transient decrease 2 h after treatment), P-Akt levels were decreased by 93.7% 2 h after treatment ($P < 0.001$). Given that expression of total HER2 and phosphorylated HER2 were reduced simultaneously by SL-1-39, we deduced that the down-regulation of total HER2, rather than merely a decrease in phosphorylation, was the primary effect of SL-1-39. To examine whether the changes in total HER2 expression were due to alterations at the transcriptional level, qRT-PCR was used to evaluate the transcript levels of HER2 in MDA-MB-453 cells
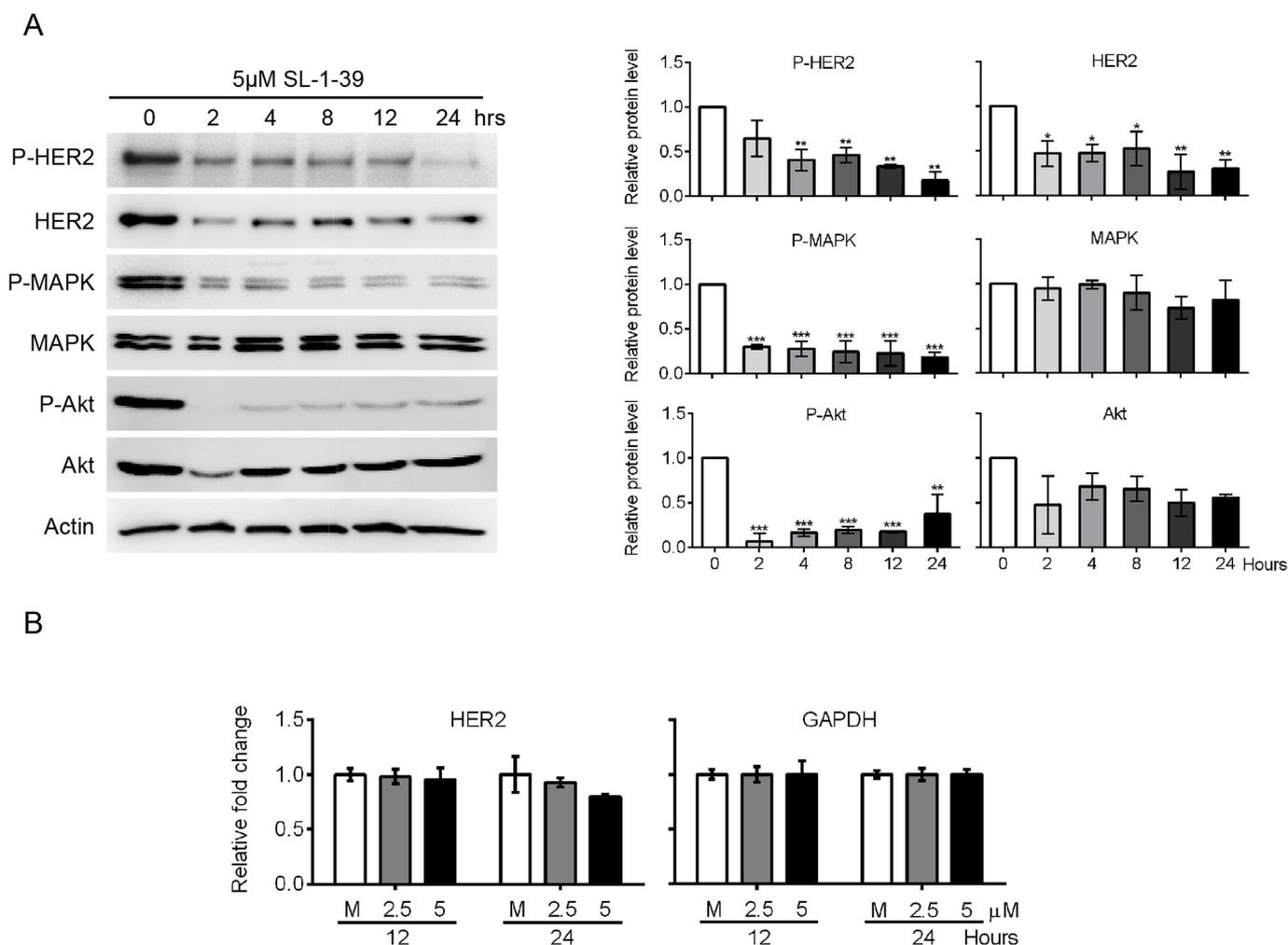
A

B

Fig. 5. **Early decrease in HER2, pMAPK and pAkt expression induced by SL-1-39 is independent of mRNA transcription.** (A) MDA-MB-453 cells were plated in 6-well plates and treated with 5 μM SL-1-39 for 2, 4, 8, 12, 24 h. HER2, p-MAPK, MAPK, p-Akt, Akt protein expressions were analyzed with western blots. Actin served as control. Quantification of western blot was performed, in which columns represent average protein expression level (with SD; *, P < 0.05; **, P < 0.01; ***, P < 0.001). (B) MDA-MB-453 cells were plated in 6-well plates and treated with 2.5 μM, 5 μM SL-1-39 or mock treated for 12 or 24 h. Real-time PCR analysis of HER2 (P > 0.05) in total RNA extracted from cell lysates were performed. GAPDH served as control.

treated as previously mentioned. Results show that there were no significant changes in HER2 mRNA levels even after 24 h of treatment with 5 μM of SL-1-39 (Fig. 5B), indicating that any changes in HER2 expression must occur post-transcriptionally.

3.4. SL-1-39 decreases HER2 levels through lysosomal degradation

In order to determine whether the decrease in HER2 levels is associated with proteasomal degradation, we blocked the function of the proteasome with varying concentrations of MG132 following treatment of MDA-MB-453 cells with 5 μM SL-1-39. HER2 protein expression was reduced by 42% when treated with SL-1-39 alone, but the presence of MG132 did not restore the decreased HER2 expression induced by SL-1-39 (Fig. 6A); whereas the expression of β-catenin, a protein known to be degraded via the proteasome, was restored in a concentration-dependent manner. This was repeated with another proteasome inhibitor, ALLN, and results were consistent with the MG132 data (Fig.S4). However, when SKBR3 cells were treated with a lysosomal inhibitor bafilomycin (BAF) after SL-1-39 treatment, HER2 expression was restored in a concentration-dependent manner, as was β-catenin (Fig. 6B). Specifically, 20 nM BAF was sufficient to return HER2 protein levels to that of control cells. To further support the notion that SL-1-39 reduces HER2 expression via lysosomal degradation, immunofluorescence

microscopy was used to monitor HER2 expression after SL-1-39 treatment in the presence and absence of BAF. As shown in Fig. 6C, immunolabeled HER2 protein levels are reduced after SL-1-39 treatment in comparison to control cells. Consistent with the western blot data, immunofluorescence of HER2 protein levels revealed that both 20 nM and 50 nM BAF was sufficient to restore HER2 protein to normal levels in cells previously treated with SL-1-39 (Fig. 6C).

We considered that if HER2 is being degraded by the lysosome, the protein would be trafficked to this organelle, and HER2 would colocalize with LAMP1, a resident lysosomal marker. Interestingly, none of our experiments showed any colocalization of LAMP1 with HER2. Instead, HER2 was only detected at the cell surface, even when total HER2 expression levels were markedly reduced by treatment with SL-1-39. These data are consistent with a model in which HER2 does traffic to the lysosome for degradation, but that the HER2 epitope recognized by the antibody is highly sensitive to lysosomal degradation, which makes concomitant detection of HER2 and LAMP1 difficult.

4. Discussion

One of the most widely used HER2-targeted therapies is trastuzumab, a monoclonal antibody that binds to and blocks HER2 dimerization, which promotes its degradation via endocytic receptor
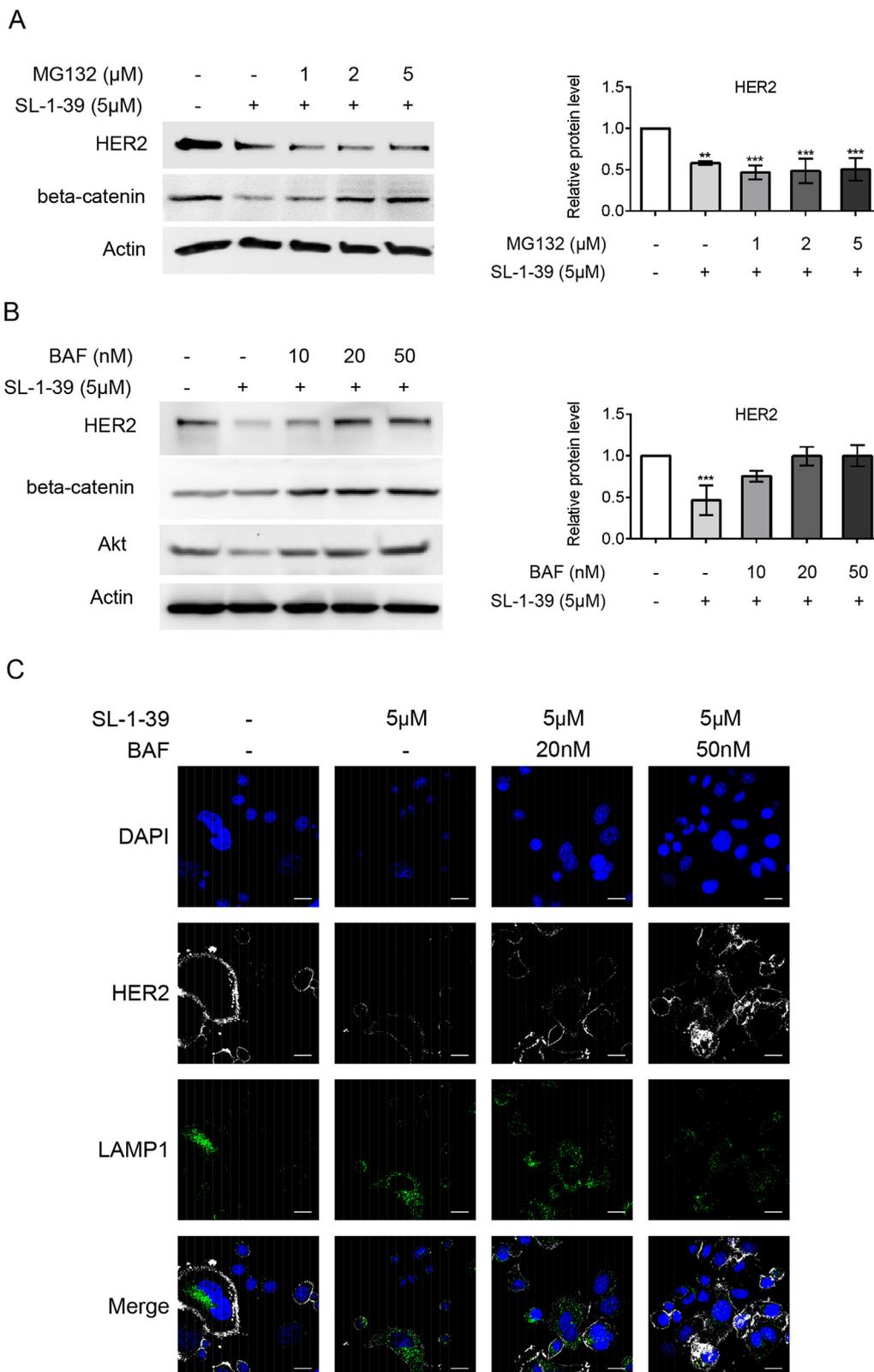
Fig. 6. SL-1-39 induced HER2 downregulation through lysosomal degradation. (A) MDA-MB-453 cells were plated in 6-well plates and treated with 5 μM SL-1-39 for 22 h then exposed with proteasome inhibitor, MG-132 for 2 h. HER2, beta-catenin protein expressions were analyzed with western blots. Actin served as control. (B–C) SKBR3 cells were treated with 5 mM SL-1-39 or mock treated. After 22 h, SL1-39 treated cells were exposed to 20 or 50 nM of bafilomycin for 2 h. (B) Cells were collected for western blot analysis or (C) fixed and analyzed on a fluorescent microscope. Nuclei were visualized by DAPI staining (in blue), HER2 and LAMP1 were stained in white and green, respectively. Scale bars represent 20 μm.

degradation [27,28]. This in turn induces the accumulation of the cyclin-dependent kinase inhibitor (CKI) p27 to promote cell cycle arrest [29–31]. Although patients with HER2+ breast cancer generally show a positive response to trastuzumab, multiple studies indicate that relapse often occurs after prolonged treatment [9,32]. The development of acquired resistance is often associated with mutations that: (1) prevent trastuzumab binding; (2) upregulate HER2 downstream signaling

pathways; (3) enhance signaling through alternate pathways; or (4) fail to trigger immune-mediated mechanisms to destroy tumor cells [33–35]. The development of resistance highlights the need to develop new therapeutic options aimed at improving outcomes of patients with HER2+ breast cancer.

SHetA2, one of the original Flex-Hets, exhibited promising growth inhibitory effects across multiple cancer types [17,19,20,22]. Previous

studies have demonstrated that SHetA2 can induce G1 cell cycle arrest by promoting proteasomal degradation of cyclin D1 in both ovarian and kidney cancer cells [36–38]. SHetA2 has also been shown to target the mitochondria, altering the expression of Bcl-2, caspase 3, and PARP-1 protein, subsequently leading to mitochondrial swelling and ultimately apoptosis [36,38,39]. A study carried out by Myers et al. found that SHetA2 is likewise capable of inhibiting angiogenesis in cancer cells [21]. Furthermore, numerous studies have reported on the relatively low to no toxicity of SHetA2, even at concentrations far exceeding its effective dose [36,40,41]. However, as the utility of SHetA2 is limited by its high lipophilicity (logP) [22], 2nd generation SHetA2 analogs were designed and synthesized to achieve a lower logP value by modifying the structure of the thiochromane ring while retaining the nitrophenyl group and the thiourea linker [22].

In this current study, we not only demonstrated the growth-inhibitory effects of the 2nd generation analog SL-1-39 on the HER2+ breast cancer cells, MDA-MB-453 and SKBR3 (Table 1), but we also demonstrated that the decrease in cell number was associated with an interruption of cell cycle progression through the down-regulation of multiple key cell cycle regulators, such as cyclin A and D1. These observations are consistent with previous studies carried out on the parental drug, SHetA2, and another 2nd generation analog, SL-1-18, both of which have been shown to decrease cyclin D1 expression and subsequently arrest cells at the G1 phase [24,36,37]. We speculate that the post-transcriptional decrease in cyclin D1 levels (see Fig. 2) is likely attributed to reduction in MAPK activity mediated by SL-1-39 treatment. Alternatively, as seen with SL-1-18, SL-1-39 may increase the degradation of the cyclin D1 protein via the proteasome and/or lysosome, although this was not observed in any of the MG132 or BAF experiments (data not shown).

The most notable results presented in this study demonstrate that SL-1-39 reduces protein expression of HER2 by inducing lysosomal degradation (Figs. 4–6). In the HER2+ breast cancer cell lines MDA-MB-453, SKBR3, T47D, and BT-474, SL-1-39 decreased HER2 protein expression and the HER2-associated phosphorylation of MAPK in a time-dependent manner (Figs. 4–5). Though HER2 protein levels decreased within 2 h of exposure (Fig. 5), HER2 mRNA levels remained unchanged, suggesting that the decrease in HER2 is associated with degradation of the HER2 protein. Curiously, we found that cells with lower levels of HER2 (e.g. T47D) were more sensitive to SL-1-39-induced HER2 degradation than cells with high levels of HER2 (e.g. SKBR3).

This is the first study to show that a flexible heteroarotinoid analog can target the HER2 signaling pathway, and our results suggest that this decrease is associated with the lysosomal degradation pathway. Such a finding is not completely without precedence, as other anti-HER2 agents, including trastuzumab, are known to bind selectively to the extracellular domain of HER2 and promote HER2 degradation by receptor-mediated endocytosis into the lysosome [29,42,43]. How SL-1-39 triggers the lysosomal degradation pathway remains unclear. However, we speculate that since the normal turnover of most plasma membrane receptors requires lysosomal targeting via the ubiquitination pathway [44], and HER2 has been shown in previous studies to undergo ubiquitin-dependent lysosomal degradation [45–47], SL-1-39 may initiate degradation of HER2 by triggering its ubiquitination. This supposition is further supported by our recently published study on the sister compound, SL-1-18, which promotes the ubiquitination and subsequent degradation of the cytoplasmic receptor ERα.

The observation that SL-1-39 down-regulates HER2 faster than trastuzumab (2 vs. 24 h, respectively) [48–51] is quite promising. Especially intriguing is the idea that SL-1-39 might be an effective therapeutic against certain trastuzumab-resistant breast cancers, particularly those that are associated with a truncated HER2 (p95-HER2) or ERBB2 mutations [52]. Since SL-1-39 works intracellularly, the lack of an extracellular domain in p95-HER2 should have little to no effect on its activity. Similarly, the most common ERBB2 mutations in breast

cancer patients do not affect the HER2 ubiquitination docking site, tyrosine-1112, which allows the polyubiquitination of HER2 via the E3 ubiquitin ligase (i.e. c-Cbl) [45]. In short, our encouraging findings warrant further development of SL-1-39 as a potential therapeutic for HER2+ breast cancer.

Conflicts of interest

All authors declare no conflicts of interest.

Acknowldegements

Appendix A. Supplementary data

Supplementary data to this article can be found online at https://doi.org/10.1016/j.canlet.2018.11.022.

References

[1] W.J. Wang, et al., Recent progress in HER2 associated breast cancer, Asian Pac. J. Cancer Prev. APJCP 16 (7) (2015) 2591–2600.

[2] S. Ahmed, A. Sami, J. Xiang, HER2-directed therapy: current treatment options for HER2-positive breast cancer, Breast Canc. 22 (2) (2015) 101–116.

[3] A.C. Wolff, et al., Recommendations for human epidermal growth factor receptor 2 testing in breast cancer: American Society of Clinical Oncology/College of American Pathologists clinical practice guideline update, J. Clin. Oncol. 31 (31) (2013) 3997–4013.

[4] J.J. Barron, et al., HER2 testing and subsequent trastuzumab treatment for breast cancer in a managed care environment, Oncol. 14 (8) (2009) 760–768.

[5] H. Yaziji, et al., HER-2 testing in breast cancer using parallel tissue-based methods, JAMA 291 (16) (2004) 1972–1977.

[6] T.J. Ballinger, M.E. Sanders, V.G. Abramson, Current HER2 testing recommendations and clinical relevance as a predictor of response to targeted therapy, Clin. Breast Canc. 15 (3) (2015) 171–180.

[7] P. den Hollander, M.I. Savage, P.H. Brown, Targeted therapy for breast cancer prevention, Front Oncol. 3 (2013) 250.

[8] A.T. Baker, A. Zlobin, C. Osipo, Notch-EGFR/HER2 bidirectional crosstalk in breast cancer, Front Oncol. 4 (2014) 360.

[9] I. Kumler, M.K. Tuxen, D.L. Nielsen, A systematic review of dual targeting in HER2-positive breast cancer, Cancer Treat Rev. 40 (2) (2014) 259–270.

[10] M. Burotto, et al., The MAPK pathway across different malignancies: a new perspective, Cancer 120 (22) (2014) 3446–3456.

[11] E.M. Ciruelos Gil, Targeting the PI3K/AKT/mTOR pathway in estrogen receptor-positive breast cancer, Cancer Treat Rev. 40 (7) (2014) 862–871.

[12] W. Tai, R. Mahato, K. Cheng, The role of HER2 in cancer therapy and targeted drug delivery, J. Contr. Release 146 (3) (2010) 264–275.

[13] D. Graus-Porta, et al., ErbB-2, the preferred heterodimerization partner of all ErbB receptors, is a mediator of lateral signaling, EMBO J. 16 (7) (1997) 1647–1655.

[14] S.T. Lee-Hoeflich, et al., A central role for HER3 in HER2-amplified breast cancer: implications for targeted therapy, Cancer Res. 68 (14) (2008) 5878–5887.

[15] F. Puglisi, et al., Current challenges in HER2-positive breast cancer, Crit. Rev. Oncol. Hematol. 98 (1) (2016) 211–212.

[16] C.C. Applegate, M.A. Lane, Role of retinoids in the prevention and treatment of colorectal cancer, World J. Gastrointest. Oncol. 7 (10) (2015) 184–203.

[17] K.H. Chun, et al., The synthetic heteroarotinoid SHetA2 induces apoptosis in squamous carcinoma cells through a receptor-independent and mitochondria-dependent pathway, Cancer Res. 63 (13) (2003) 3826–3832.

[18] S. Liu, et al., Synthesis of flexible sulfur-containing heteroarotinoids that induce apoptosis and reactive oxygen species with discrimination between malignant and benign cells, J. Med. Chem. 47 (4) (2004) 999–1007.

[19] D.M. Benbrook, et al., Flexible heteroarotinoids (Flex-Hets) exhibit improved therapeutic ratios as anti-cancer agents over retinoic acid receptor agonists, Invest. N. Drugs 23 (5) (2005) 417–428.

[20] T. Liu, et al., Flex-Hets differentially induce apoptosis in cancer over normal cells by directly targeting mitochondria, Mol. Canc. Therapeut. 6 (6) (2007) 1814–1822.

[21] T. Myers, et al., Flexible heteroarotinoid (Flex-Het) SHetA2 inhibits angiogenesis in vitro and in vivo, Invest. N. Drugs 27 (4) (2009) 304–318.

[22] S. Liu, et al., Synthesis and evaluation of the diarylthiourea analogs as novel anti-cancer agents, Bioorg. Med. Chem. Lett 25 (6) (2015) 1301–1305.

[23] Y. Zhang, et al., High performance liquid chromatographic analysis and preclinical pharmacokinetics of the heteroarotinoid antitumor agent, *SHetA2*, Cancer Chemother. Pharmacol. 58 (5) (2006) 561–569.

[24] M.M. Fallatah, et al., Novel flexible heteroarotinoid, SL-1-18, promotes ERalpha

degradation to inhibit breast cancer cell growth, Cancer Lett. 408 (2017) 82–91.

[25] V. Cryns, J. Yuan, Proteases to die for, Genes Dev. 12 (11) (1998) 1551–1570.

[26] M. Poreba, et al., Caspase selective reagents for diagnosing apoptotic mechanisms, Cell Death Differ. (2018).

[27] J.S. Ross, et al., The HER-2 receptor and breast cancer: ten years of targeted anti-HER-2 therapy and personalized medicine, Oncol. 14 (4) (2009) 320–368.

[28] L. Dean, Trastuzumab (herceptin) therapy and ERBB2 (HER2) genotype, in: V. Pratt, et al. (Ed.), Medical Genetics Summaries, National Center for Biotechnology Information (US), Bethesda (MD), 2012.

[29] M. Luque-Cabal, et al., Mechanisms behind the resistance to trastuzumab in HER2-amplified breast cancer and strategies to overcome it, Clin. Med. Insights Oncol. 10 (Suppl 1) (2016) 21–30.

[30] X.F. Le, F. Pruefer, R.C. Bast Jr., HER2-targeting antibodies modulate the cyclin-dependent kinase inhibitor p27Kip1 via multiple signaling pathways, Cell Cycle 4 (1) (2005) 87–95.

[31] J. Baselga, et al., Mechanism of action of trastuzumab and scientific update, Semin. Oncol. 28 (5 Suppl 16) (2001) 4–11.

[32] M.S. Mohd Sharial, J. Crown, B.T. Hennessy, Overcoming resistance and restoring sensitivity to HER2-targeted therapies in breast cancer, Ann. Oncol. 23 (12) (2012) 3007–3016.

[33] S. Loi, et al., Tumor infiltrating lymphocytes are prognostic in triple negative breast cancer and predictive for trastuzumab benefit in early breast cancer: results from the FinHER trial, Ann. Oncol. 25 (8) (2014) 1544–1550.

[34] S. Loi, et al., Tumor PIK3CA mutations, lymphocyte infiltration, and recurrence-free survival (RFS) in early breast cancer (BC): results from the FinHER trial, J. Clin. Oncol. 30 (15_suppl) (2012) 507-507.

[35] P.R. Pohlmann, I.A. Mayer, R. Mernaugh, Resistance to trastuzumab in breast cancer, Clin. Canc. Res. 15 (24) (2009) 7479–7491.

[36] T. Liu, et al., Development of flexible-heteroarotinoids for kidney cancer, Mol. Canc. Therapeut. 8 (5) (2009) 1227–1238.

[37] C.P. Masamha, D.M. Benbrook, Cyclin D1 degradation is sufficient to induce G1 cell cycle arrest despite constitutive expression of cyclin E2 in ovarian cancer cells, Cancer Res. 69 (16) (2009) 6565–6572.

[38] K.D.B. Baskar Nammalwar, Richard A. Bunce, SHetA2 – a mini review of a promising anticancer drug, JSM Chemistry 1 (1) (2013).

[39] Y. Lin, et al., Involvement of c-FLIP and survivin down-regulation in flexible heteroarotinoid-induced apoptosis and enhancement of TRAIL-initiated apoptosis in lung cancer cells, Mol. Canc. Therapeut. 7 (11) (2008) 3556–3565.

[40] K.K. Kabirov, et al., Oral toxicity and pharmacokinetic studies of SHetA2, a new chemopreventive agent, in rats and dogs, Drug Chem. Toxicol. 36 (3) (2013) 284–295.

[41] R.S. Doppalapudi, et al., Genotoxicity of the cancer chemopreventive drug candidates CP-31398, SHetA2, and phospho-ibuprofen, Mutat. Res. 746 (1) (2012) 78–88.

[42] C.A. Hudis, Trastuzumab–mechanism of action and use in clinical practice, N. Engl. J. Med. 357 (1) (2007) 39–51.

[43] M. Barok, H. Joensuu, J. Isola, Trastuzumab emtansine: mechanisms of action and drug resistance, Breast Canc. Res. 16 (2) (2014) 209.

[44] M.J. Clague, S. Urbe, Ubiquitin: same molecule, different degradation pathways, Cell 143 (5) (2010) 682–685.

[45] X. Li, et al., Degradation of HER2 by Cbl-based chimeric ubiquitin ligases, Cancer Res. 67 (18) (2007) 8716–8724.

[46] C. Marx, et al., ErbB2 trafficking and degradation associated with K48 and K63 polyubiquitination, Cancer Res. 70 (9) (2010) 3709–3717.

[47] J. Nunes, et al., ATG9A loss confers resistance to trastuzumab via c-Cbl mediated Her2 degradation, Oncotarget 7 (19) (2016) 27599–27612.

[48] T. Kute, et al., Development of Herceptin resistance in breast cancer cells, Cytometry 57 (2) (2004) 86–93.

[49] D. Kostyal, et al., Trastuzumab and lapatinib modulation of HER2 tyrosine/threonine phosphorylation and cell signaling, Med. Oncol. 29 (3) (2012) 1486–1494.

[50] M.A. Molina, et al., Trastuzumab (herceptin), a humanized anti-Her2 receptor monoclonal antibody, inhibits basal and activated Her2 ectodomain cleavage in breast cancer cells, Cancer Res. 61 (12) (2001) 4744–4749.

[51] C.D. Austin, et al., Endocytosis and sorting of ErbB2 and the site of action of cancer therapeutics trastuzumab and geldanamycin, Mol. Biol. Cell 15 (12) (2004) 5268–5282.

[52] Z. Ping, et al., ERBB2 mutation is associated with a worse prognosis in patients with CDH1 altered invasive lobular cancer of the breast, Oncotarget 7 (49) (2016) 80655–80663.